THE MECHANICAL STIMULI CONTROL SYSTEM: ENHANCING THE REPLICATION OF MECHANICAL ENVIRONMENTS ASSOCIATED WITH VASCULAR DISEASE IN ENDOTHELIAL CELL STUDIES

An Undergraduate Research Scholars Thesis

by

MICHAEL J. DRAPER

Submitted to Honors and Undergraduate Research
Texas A&M University
in partial fulfillment of the requirements for the designation as an

UNDERGRADUATE RESEARCH SCHOLAR

Approved by
Research Advisor: Dr. Michael R. Moreno

May 2015

Major: Biomedical Engineering

TABLE OF CONTENTS

ABSTRACT

Stress Angle Device: Reproducing the Mechanical Environments Associated with Vascular Disease in Endothelial Cell Studies. (May 2015)

Michael J. Draper
Department of Biomedical Engineering
Texas A&M University

Research Advisor: Dr. Michael R. Moreno
Department of Mechanical Engineering

Atherosclerosis is a common form of cardiovascular disease – the leading cause of death in the United States. Although previous cell studies have explored responses to cyclic stretch and fluid shear stress, orientation of these two parameters have only been orthogonal to one another, which replicates the non-atherogenic conditions of a straight, unbranched vascular segment. However, in tortuous vessels or bifurcations, CFD analysis of flow patterns reveals that pro-atherogenic regions of vasculature exhibit non-perpendicular orientations of cyclic stretch and fluid shear stress, with some discrete spatial angle between the two. The Vascular Stress Angle Device (VSAD) is an *in vitro* system that replicates the mechanical environments seen *in vivo* where pro-atherogenic conditions exist (e.g. carotid bifurcation). This study describes the progressive development of the Mechanical Stimuli Control System (MSCS) used by the VSAD to enhance fluid shear stress and cyclic stretch control. The MSCS satisfied 5 out of 6 validation requirements, indicating its pending success in recreating physiological and pathological vascular mechanical environments. By replicating these conditions, the VSAD may serve as a useful tool in studies of the progression of atherosclerosis and therapeutic interventions for pro-atherogenic pathologies.

DEDICATION

I dedicate this research to my parents. Without their continued support this opportunity would not have been possible.

ACKNOWLEDGEMENTS

I would like to thank Dr. Michael R. Moreno for giving me the opportunity to work in his lab. By giving me this opportunity, I have discovered a love for scholarly research I would have otherwise not had the opportunity to explore.

NOMENCLATURE

CVD	Cardiovascular Diseases
EC	Endothelial Cells
FSS	Fluid Shear Stretch
CS	Cyclic Stretch
SA	Stress Angle
VSAD	Vascular Stress Angle Device
MSCS	Mechanical Stimuli Control System
BFW	Blood Flow Waveform

CHAPTER I

INTRODUCTION

Atherosclerosis

Cardiovascular diseases (CVDs) are the leading cause of death in the United States, with over 780 thousand deaths annually [1]. Approximately 32% of all deaths can be attributed to CVDs, and the National Institute of Health has recorded over 83 million prevalent cases of CVDs [2]. The impact of cardiovascular disease on the economy is evidenced in the total direct and indirect costs associated with these diseases, which amounted to $313 billion and 16.8% of all economic costs of illnesses in 2009 [3].

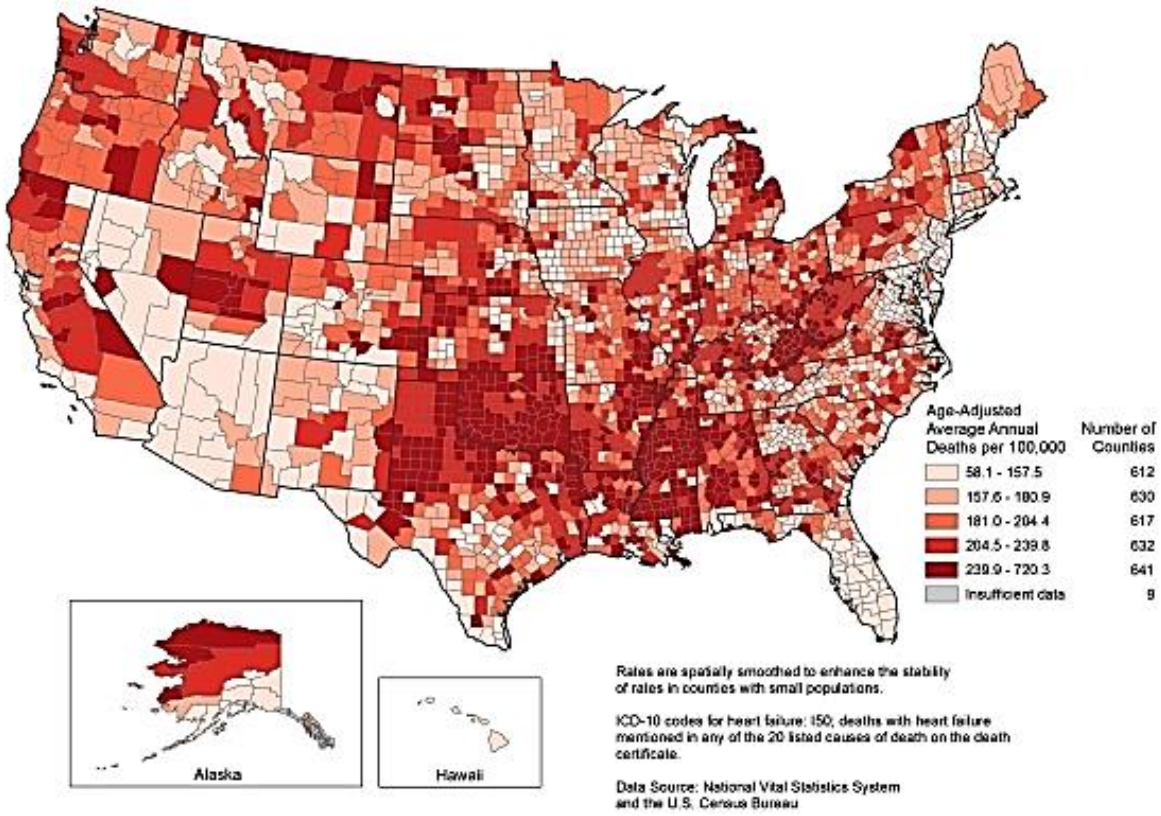

Figure 1. A map showing death rates related to cardiovascular disease across the United States between 2007 and 2009 **[4]**.

The most common form of CVDs is atherosclerosis – the narrowing and hardening of arteries due to the buildup of plaque. Atherosclerosis is localized at branch points and curvatures in the arterial tree – where complex flow is observed. The mechanical environments of these pro-atherogenic regions differ greatly from the mechanical environment of pressure-driven flow through a straight tube, which can be used to describe the majority of the vasculature [5, 6].

Endothelial Cell Studies

Mechanical factors, such as low mean and oscillating fluid shear stress, have been correlated with intimal thickening in the carotid bifurcation and the abdominal aorta [5, 7]. Thus, it has been hypothesized that mechanical stimuli may induce endothelial cell (EC) responses that are pro-atherogenic. If the physiological processes that take place in atherosclerosis as a response to the mechanical environment can be exposed, there may be a greater potential for the development of therapeutic interventions to halt the progression of the disease.

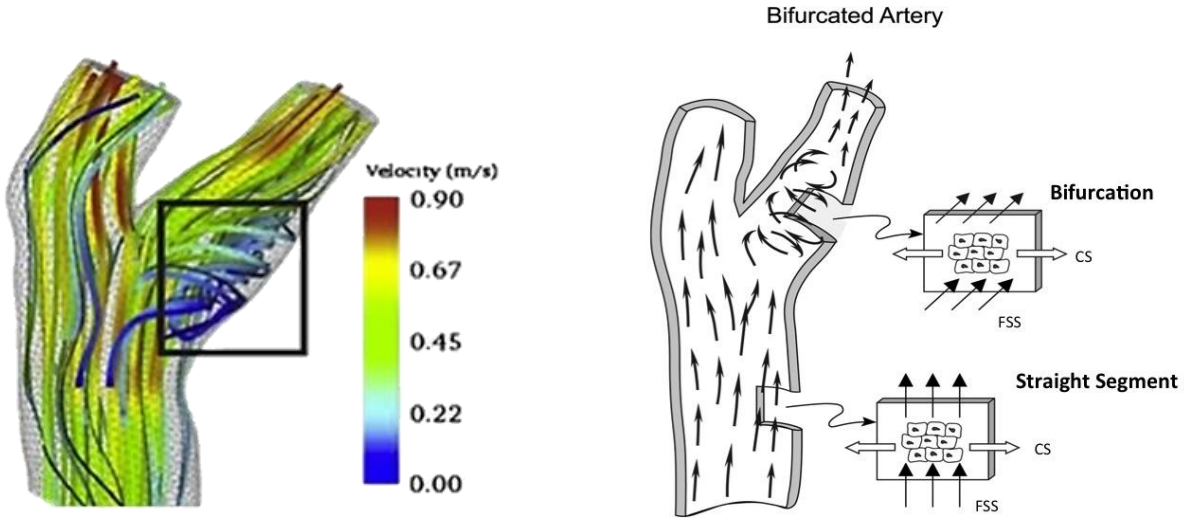

Figure 2. Flow streamlines in a carotid bifurcation with 50% stenosis. A significant helical component of flow can be observed in the boxed area (Left) **[5]**. Blood flow through a straight arterial segment translates to a perpendicular relationship between FSS and CS; however, a non-perpendicular relation exists in branched or tortuous segments. (Right) **[8]**

A variety of methods have been used in previous studies to observe the effects of varying EC shear stresses and strains on cellular proliferation, apoptosis, migration, permeability, and remodeling [9, 10]. Some studies have combined these methods to observe how ECs respond to the simultaneous application of both fluid shear stresses (FSSs) and cyclic stretches (CSs) [11]. Two commonly used methods for observing EC response to simultaneous FSS and CS are the explanted vessel and mock artery methods [12, 13]. The former method utilizes a blood vessel perfused to a flow system, while the latter uses a constructed compliant tube with similar dimensions to a vessel and cells seeded on the inner surface.

While the methods described above have provided many researchers with a greater understanding of EC mechanotransduction, their utility is limited by the fact that they cannot be used to recreate the complex mechanical environments found in pro-atherogenic regions of vasculature. Previous literature fails to address the effect helical flow has on endothelial cell mechanotransduction. The fluid velocity vector has a substantial circumferential component and therefore shear stresses in this region are not exclusively in the axial direction (see **Figure 2**), as they would be in a straight tube. Davis et al. (2014) defines the "Stress Angle" (SA) as the spatial angle between FSS and CS [8], as opposed to the "Phase Angle" (PA) which is the temporal angle between the previously mentioned stimuli [14]. Given that the stress angle varies in regions where disease typically forms, it is important to develop the ability to investigate these conditions.

The Vascular Stress Angle Device

To observe the role that the SA plays in replicating the pro-atherogenic mechanical environments seen in tortuous vessels, the Vascular Stress Angle Device (VSAD) was developed. The device was designed to provide physiologic levels of FSS and CS to an attached cell-seeded membrane at varying angles, while maintaining a sterile, nourishing environment for the cells to survive in. The design inputs for the VSAD were: (a) the device had to be capable of subjecting cultured ECs to FSS of physiologically relevant magnitude, (b) the device had to be capable of subjecting the cells to a uniaxial stretch of physiologically relevant magnitude, (c) the device had to allow the angle between the fluid shear stress and the uniaxial stretch to be varied in 15° increments from 0 - 90°, (d) the device had to facilitate control of the PA, and (e) the device had to enable bright field and confocal microscopy of the cells in the device.

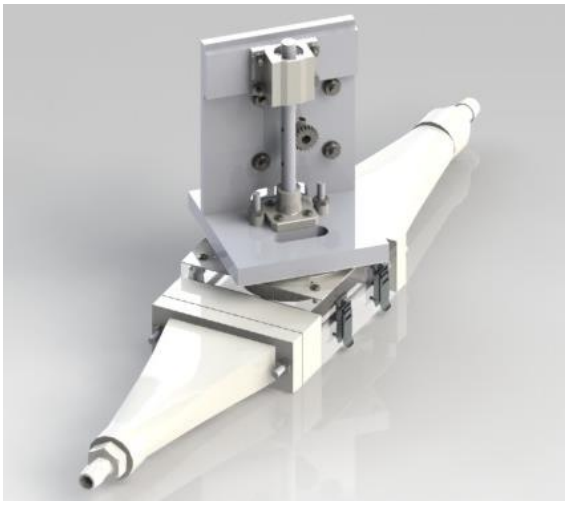

Figure 3. A Dassault Systèmes SOLIDWORKS model of the Stress Angle Device. The apparatus consists of a parallel plate flow chamber for applying FSS to an endothelial cell membrane and a rotatable motor for applying CS to the cells at various SA states.

The selected method of controlling FSS in the VSAD was based on a modified version of the parallel plate flow system described in a 1971 study [15]. In the modified design, a cell-seeded silicone membrane lines the top plate of the chamber. As described in a 2014 review article by

Davis et al., the shear stress applied by the fluid at the wall of a parallel plate flow chamber can be calculated from the Navier-Stokes equations and continuity equation for the system [8]. Assuming steady, fully developed, laminar flow of a Newtonian fluid, the expression for FSS at the membrane in the parallel plate chamber is

$$\mathrm{FSS} = \frac{6\,\mu\,\mathrm{Q}}{\mathrm{wh}^2} \qquad (1)$$

where Q is the volumetric flow rate, μ is the fluid dynamic viscosity, w is the flow channel width, and h is the flow channel height. By assuming Poiseuille flow in the parallel plate chamber, the flow rate may be adjusted by a pump to achieve shear stresses that are physiologically relevant.

To control the flow rate through the VSAD it must be attached to a flow loop, which includes a gear pump (Ismatec, MV 7617-70) driven by signals output from a function generator (BK Precision, 4017A). An intravascular pressure transducer (Millar, Mikro-Tip Catheter Transducer) was used to monitor pressure in the system, and flow rates were monitored using a Transonic clamp-on ultrasonic flow probe (Transonic, ME 7PXL) connected to a TS410 Transonic Flow Meter. Outputs from the flow meter and pressure transducer were routed to a National Instruments DAQ device (National Instruments, BNC-2110 enabled by a USB-6251), where they were sampled and sent to the LabVIEW-enabled laptop for graphical display and feedback for controlling parameters. As done in previous studies, a pulse dampener was added to the flow loop to replicate the effects of energy storage in elastic arteries [7]. It is believed that dampening the gear pump's sinusoidal flow output makes the flow waveform more representative of

vascular blood flow. A valve is also added to the flow loop to adjust the system pressure and replicate resistance in downstream vasculature, as per previous studies.

Both ends of the cell-seeded silicone membrane attach to a custom clamp driven by a stepper motor (Anaheim Automation). The stepper motor is able to cyclically apply physiologically relevant strain to the cell-seeded membrane. With the motor and membrane mounted on a rotatable stage, which is inserted into the top plate of the flow chamber, the tester is capable of rotating the membrane in 15° increments to achieve various SA states. A glass microscope slide was installed on the bottom plate so that an inverted microscope may observe the membrane during testing. Flow straighteners were installed at the inlet and outlet of the device to reduce turbulence.

A 1994 study by Moore et al. used 8 ± 4 dynes/cm^2 as a target FSS to represent pro-atherogenic conditions [7]. Therefore, since the Moore et al. study is considered to be a standard for these studies, the VSAD needed to be able to subject ECs to this FSS at 1 Hz, as well as a 5% CS at a rate of 1 Hz as implemented by the stepper motor. Testing needed to be viable for 24 hours at 15° SA positions between the range of 0 - 90°.

Preliminary studies using the VSAD validated some of its design concepts by demonstrating that ECs may remain attached to Sylgard membranes at pro-atherogenic FSSs; however, these studies also exposed critical flaws in the design of the VSAD. Many of these flaws were attributable to the method of controlling the FSS and CS. Shortcomings of the FSS and CS control method were: (1) inability to quantitatively control the temporal PA between FSS and CS, (2) imprecise

control of desired FSS attributed to guess-and-check operation of function generator control signals, (3) limited replication of CS in the form of a sinusoidal, square, triangle, or sawtooth waveform, and (5) complex operation of CS control, which required a C-based programming language to specify motor commands, making it difficult to use. Thus, a new system had to be designed that would address these flaws by tailoring design inputs to make the VSAD more controlled and thus more useful in endothelial cell studies.

CHAPTER II

METHODS

Design Inputs

To improve the method of controlling FSS and CS, a new series of design inputs had to be developed based on the existing requirements and observed flaws from preliminary testing (Table 1). A series of tests were explicitly defined for verifying each design input, which provided direction for system development.

Table 1.

Design Inputs	Test
Enabled via visual programming language	The system must be implemented using LabVIEW
Contour control for CS	System must be able to accept two different sets of discrete data points and fit a curve for operation of the motor.
Real time FSS control	Within 10 seconds of a user increasing the steady or unsteady flow rate by 50 mL/min, it must increase by at least 20 mL/min.
Automated Feedback-enabled flow waveform fine-tuning	Within 10 minutes, the system must use feedback from the flow meter to automatically match user-defined flow parameters within ± 5 mL/min.
Continuous system operation	The system must apply both stress and strain continuously for 24 hours at a specified input parameter value
Temporal PA control	Temporal PA between FSS and CS must be controllable within ± 10 degrees of input phase angle

System Development

With the design inputs and verification tests clearly specified, development of the new Mechanical Stimuli Control System (MSCS) began. The MSCS consists of a CS subsystem and a FSS subsystem. These two subsystems were designed to be consolidated in a single program to control both mechanical stimuli simultaneously at a given temporal PA.

First, it was decided that the MSCS would be entirely implemented with LabVIEW (National Instruments). LabVIEW is a system design platform and development environment that uses a visual programming language. Whereas the previous system required programming knowledge for both C (for the motor controlling CS) and LabVIEW (for acquiring and displaying the outputs of the flow meter and pressure transducer), the MSCS would only require knowledge of LabVIEW.

The Cyclic Stretch Subsystem

Based on the decision to use LabVIEW, the Anaheim Automation motion system was replaced with National Instruments Motion Control products to control the CS subsystem. The new motion control system consisted of a NEMA 23 stepper motor (National Instruments, T21NRLH) controlled by a cRIO controller/chassis combination (National Instruments, cRIO-9075) via an axis stepper drive interface module. The cRIO controller connected to a LabVIEW-enabled laptop via Ethernet connection, allowing the motor output to be controlled by LabVIEW. A quadrature encoder (National Instruments, 15T-01SA-1000) was also installed to track the movement of the motor.

The new LabVIEW program for CS control was a contour movement program, which required a user-defined table of set points to specify movement. A Catmull-Rom spline was used to ensure the spline path passed through the provided points. This program allowed the user to input more complex waveforms for CS that may be more physiologically accurate (e.g. aortic blood flow) than standard waveforms (e.g. square, triangular).

For both programs to achieve a desired percent stretch for CS, the mathematical relationship between the motor movement and the percent stretch had to be determined. Stretch of an object can be expressed as

$$\mathrm{E} = \frac{\Delta L}{L_o} \times 100 \qquad (2)$$

where E is the percent stretch, ΔL is the change in length, and L_o is the initial length (4.5 inches) of the membrane. Because the shaft attaches to both ends of the membrane, any displacement of the shaft (e.g. "x" inches) will produce twice as much change in the length of the membrane (e.g. "2x" inches). The spur gear used to displace the shaft, embedded with a mating gear rack, has a 0.625" pitch diameter; implying a ratio of 1.96" of shaft displacement per motor revolution. The motor is configured for 5,000 microsteps per revolution. With this information, Equation 2 can be adjusted to express the number of steps required to achieve a certain percent stretch of the membrane:

$$57.398\,\mathrm{E} = \mathrm{N} \qquad (3)$$

where *N* is the number of microsteps required to achieve the percent stretch *E*. This relationship was used to define data tables of set points for contour motion.

The Fluid Shear Stress Subsystem

With the CS subsystem complete, development began on the FSS subsystem of the MSCS. Controlling the flow rate through the VSAD with LabVIEW required a new program that utilized the analog output function of the DAQ device to send generated signals to the gear pump. This program also had to retain the ability to acquire and display flow rate and pressure transducer data.

The gear pump is controlled by inputs ranging from 0-5 volts, where 5 volts induces the pump's maximum flow rate; however, changes in other components of the flow loop may result in different flow rates, even if they use the same pump input voltage. Such changes include adjusting the height of the pulse dampener and changing the resistance valve. To account for these changes, a calibration procedure was required. By plotting a series of input voltages against the resulting measured flow data, a linear regression was determined. This linear regression was used to convert a user-input flow rate to a corresponding signal for the pump.

The FSS subsystem of the MSCS had to enable real-time control of the pulsatile frequency and steady and unsteady components of flow. Once the flow rate inputs were converted to pump voltage values using the linear regression, they were inputted to a "Build Waveform" function that generated a sinusoidal waveform with these parameters. This constructed waveform was

sent to a second function that sent the signal from DAQ device to the pump. To enable real-time control of these parameters, the function was placed inside a while loop.

Even with calibration procedures, pump outputs can sometimes be inaccurate relative to the user input. To fine-tune the pump signal and improve its accuracy, a feedback loop was implemented using data from the flow meter. This feedback loop incrementally decreased or increased the pump voltage depending on whether the measured flow rate was greater or less than the user input. It was used to fine-tune both the steady and unsteady components of flow.

Temporal Phase Angle Control

In the original concept for controlling temporal PA, the CS and FSS subprograms would be combined into a single program. This would enable their simultaneous execution (or at least a consistent time delay between them), allowing for phase to be controlled by introducing a timed delay between the executions of the two subprograms. Unfortunately, the equipment previously described for controlling CS and FSS made this concept impossible to implement. Because the motion control devices and the DAQ device ran on two separate drivers, they could not be run together on the same program. Alternative methods to implement temporal PA in future iterations of the device will be discussed in Chapter VI.

Testing

The MSCS was subjected to the verification tests described in Table 1. To demonstrate contour control of CS, 10 second sinusoidal and sawtooth signals with amplitude 5% stretch were input as data tables. The encoder measured the motor response, which was graphically displayed on

the program front panel. Passing this test required the motor response to match the input data at each point within ± 20 steps.

Real time FSS control required the flow rate to increase by at least 20 mL/min within 10 seconds of increasing the input by 50 mL/min. This had to be demonstrated for both steady and unsteady flow. To demonstrate steady flow responsiveness, the unsteady component was set at 25 mL/min and the steady component was increased from 50 mL/min to 100 mL/min. To demonstrate unsteady flow responsiveness, the steady component was set to 150 mL/min and the unsteady component was increased from 50 mL/min to 100 mL/min. A stopwatch was used to measure the amount of time required to observe a change of 20 mL/min, as indicated by real-time displays of flow rate mean and amplitude measurements.

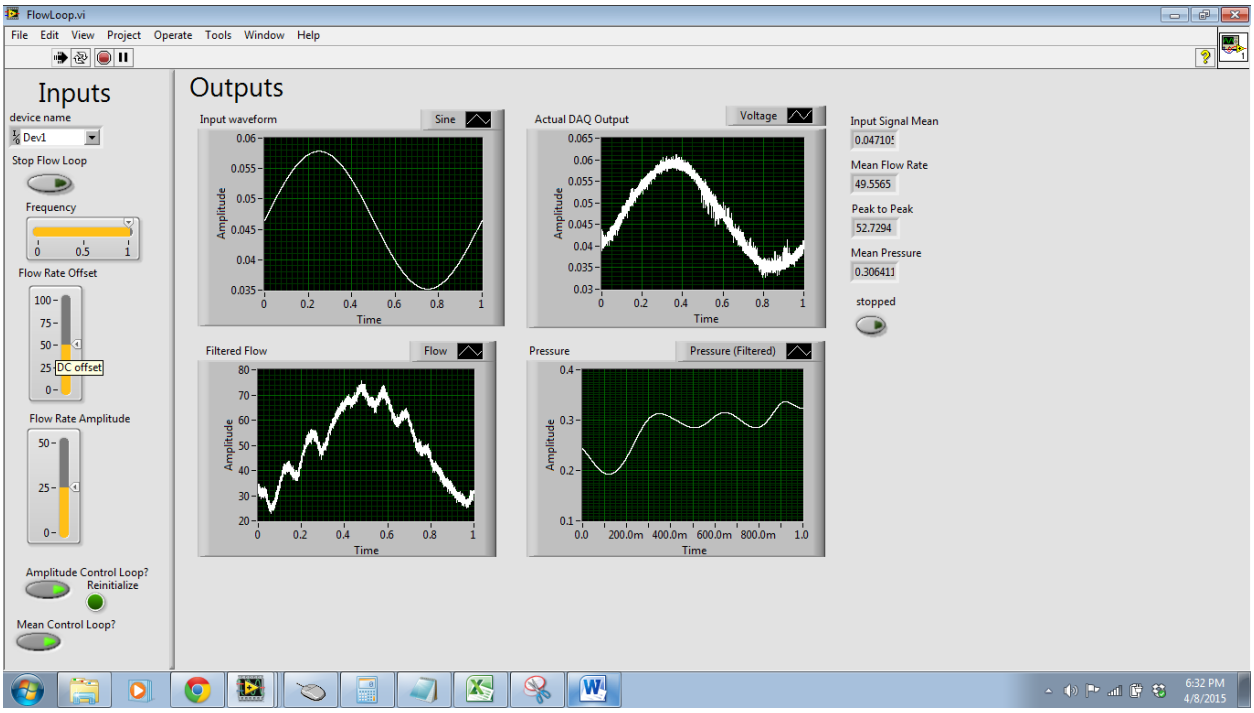

Figure 4. To test the responsiveness of the steady component of flow to new user input, the flow rate was first set at 50 mL/min ± 25 mL, as shown here. The steady flow rate input (or the flow rate offset) was then changed from 50 to 100 mL/min, and the time required for the mean flow rate (shown to the right of the graphical waveform displays) to increase from 50 to 70 mL/min was timed with a stopwatch.

To demonstrate automated feedback-enabled fine-tuning of the flow waveform, the steady and unsteady flow rates were changed in the same way as previously described for testing real-time response. The time it took for the flow rates to reach an accuracy of ± 5 mL/min of the target was recorded for both the unsteady and steady components of flow.

Both the CS and FSS programs were executed simultaneously and left to run for 24 hours to demonstrate continuous system operation. A video camera recorded the shaft movement and flow rate measurement. If the shaft stopped moving or the flow rate significantly dropped at any point in the 24 hours, the MSCS did not pass the test.

CHAPTER III

RESULTS

The MSCS was completed according to specifications, and passed all but one of the verification tests previously described.

Table 2.

Design Inputs	Test	Results
Enabled via visual programming language	The system must be implemented using LabVIEW	Pass
Contour control for CS	System must be able to accept two different sets of discrete data of points and fit a curve for operation of the motor. Observed motion must match the data within ± 20 steps.	Pass
Real time FSS control	Within 10 seconds of a user increasing the steady or unsteady flow rate by 50 mL/min, it must increase by at least 20 mL/min.	Pass
Automated feedback-enabled fine-tuning of flow waveform	Within 10 minutes, the system must use feedback from the flow meter to automatically match user-defined flow parameters within ± 5 mL/min.	Pass
Continuous system operation	The system must apply both stress and strain continuously for 24 hours at a specified input parameter value	Pass
Temporal PA control	Temporal PA between FSS and CS must be controllable within ± 10 degrees of input phase angle	Fail

The need for C-based programming was eliminated from the CS component of the MSCS. All motion control programming was hosted on LabVIEW, enabled by the use of National Instruments Motion Control products.

A graphical display of the encoder measurements for the two motion profiles demonstrated success in replicating the sinusoidal and sawtooth waveforms (see **Figure 5**). Further analysis demonstrated that the tracked movement was within ± 20 steps of each data point from the table, for both waveforms. Thus, the MSCS successfully demonstrated contour control for CS.

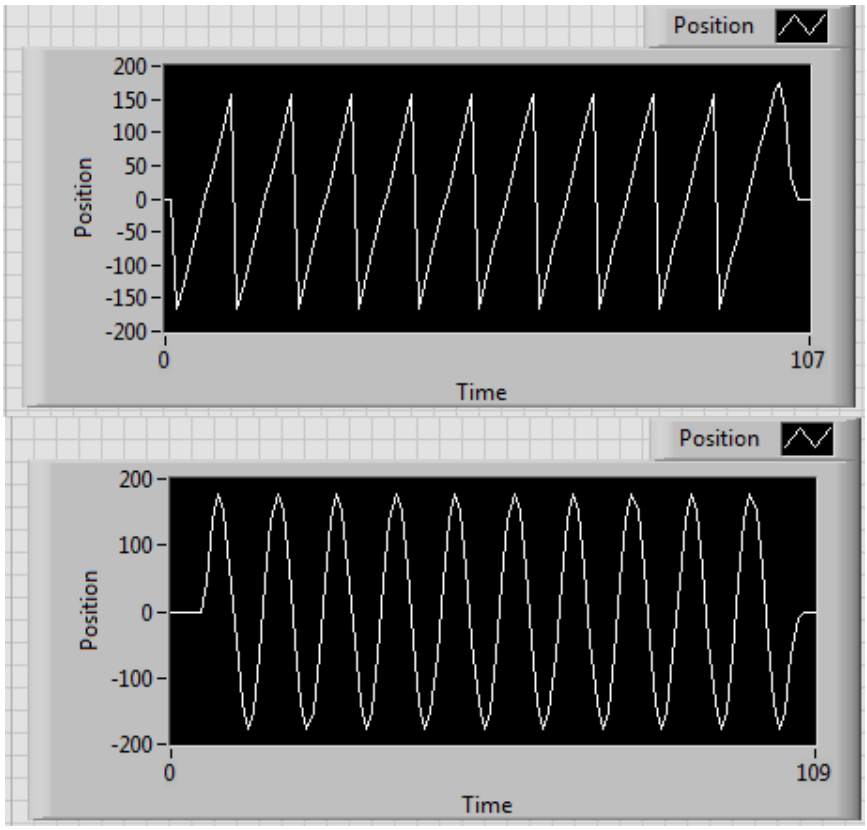

Figure 6. The two contour data sets yielded observably different waveforms. The measured positions of the sawtooth waveform (top) and sinusoidal waveform (bottom) were both within ± 20 steps of the input data points at each corresponding temporal location.

The time for the steady flow to increase from 50 to 70 mL/min was approximately 7.46 seconds. For the unsteady flow rate, it was approximately 6.16 seconds. Because both times were under 10 seconds, the MSCS successfully demonstrated real time FSS control.

The steady flow rate increased from 50 to 95 mL/min in approximately 10 seconds, suggesting that proper calibration played a larger role in accuracy than the feedback loop did. For the unsteady flow rate, it was approximately 3 minutes and 34 seconds. Because both times were under 10 minutes, the MSCS successfully demonstrated automated feedback-enabled fine-tuning of the flow waveform.

When left to run simultaneously for 24 hours, neither the FSS nor CS programs stopped or behaved unexpectedly. Thus, the MSCS successfully demonstrated continuous system operation.

Because the FSS and CS subsystems could not be consolidated in a single program, the MSCS failed to demonstrate control of the temporal PA.

CHAPTER IV

CONCLUSION

Shortcomings and Potential Improvements

The biggest shortcoming of the MSCS is the inability to replicate temporal PAs between FSS and CS.

Here, the term phase is the time-variant angle often referred to as instantaneous phase [16]. For this application, only the horizontal-axis (i.e. temporal-variant) of our waveforms needs to be discussed. Here, we will describe the phase of a wave as it refers to a sinusoidal function:

$$x(t) = A \times \cos(2\pi f t + \varphi) \quad (4)$$

where $x(t)$ is the waveform, A is the amplitude, f is frequency, t is time, and φ is phase. There are two alternatives for addressing this shortcoming, the first of which is to purchase new compatible equipment. A valuable aspect of the cRIO controller used in the CS subsystem is its modularity, which enables it to assume functions other than motor control. Introducing new functionality for the cRIO controller is as simple as inserting new modules. Two modules (National Instruments, NI 9215 and NI 9263) have been identified that provide analog input and output capabilities, effectively eliminating the need for the DAQ device. Because these two modules would use the same driver as the module currently used for the CS subsystem, compatibility issues would be eliminated. The two subprograms could be called in a single

MSCS master program that controls temporal PA by introducing time delays between CS and FSS subprogram executions.

Although the two subprograms could not be started simultaneously in a single program, they were able to run simultaneously as individual programs. Thus, the second alternative for controlling the time-variant PA between FSS and CS requires the ability to start one program consistently at some principal phase value relative to the waveform produced by the other program. In other words, the temporal PA must be consistent when no time delays are programmed. This would enable the introduction of some phase offset of "φ " before execution of the second program.

A Hall magnetic sensor connected to an analog input channel on the DAQ device and a neodymium magnet could be used to trigger the execution of the FSS program in response to a specific point in the shaft movement waveform. With the start of the FSS program occurring consistently at a constant phase relative to the shaft movement waveform, changing the temporal PA could be accomplished in the FSS program by inserting a user-defined time delay between the triggered start of the program and the actual waveform generation.

Other than temporal PA control, the MSCS was developed according to the design inputs and passed all verification tests defined in Table 1. Although it may be considered a success in this regard, many features could be added to the MSCS in future generations to improve it. One such feature would be a more accurate measurement of the stretch, taking into account spatial effects. In the current design, stretch is approximated relative to shaft displacement using Equation 2.

This approximation assumes uniform uniaxial stretch across the width of the silicone membrane, but this represents an extremely ideal scenario. In reality, stretch is variable across different spatial locations on the membrane surface, as evidenced by a reduction in width during elongation. Studies have demonstrated that percent stretch can be accurately measured spatially in silicone membranes by measuring relative marker displacements on the membrane surface [17].Two-dimensional Delauney triangulation, accompanied with other calculations, may provide an effective measure of stretch at multiple spatial locations on the membrane, providing a greater understanding of the actual stretches induced by the CS subsystem.

System Impact

The MSCS is a vital part of the VSAD, and provides greater control of the replicated mechanical environment than the previous system. Noticeable improvements can be observed in generating required flow conditions – a process which previously required minutes of painfully minute adjustments to a function generator output. Users may now directly input a numerical value for steady and unsteady flow rates to quickly achieve flow conditions with a high degree of accuracy. Improvements are also evident in the execution of stretch profiles, which were previously limited to a sinusoidal or triangular profile. Membrane stretch could now be made more representative of physiologic vascular stretch patterns by using a custom-made discrete set of points to control motion. Control of the temporal PA – a functionality previously impossible – is now realizable by introducing new modules or incorporating a Hall magnetic sensor. Finally, the whole system is consolidated to two programs and one programming language, making it more learnable and easy to interact with.

With an improved system to control mechanical stimuli, the VSAD can be more effective in its mission to replicate pro-atherogenic conditions for EC studies. The enhanced control of mechanical stimuli offered by the MSCS reduces the potential for error and increases the quality of future EC study results.

The Future of the Vascular Stress Angle Device

With the development of the MSCS, focus is now on implementing the VSAD in EC studies. The first of such studies may observe measurement the morphological adaptation of endothelial cells in response to various SA states. Significant changes to the morphology of the cells may indicate underlying pro-atherogenic cellular chemical responses to certain SAs. Further studies may observe protein expression and other responses to various SAs. Hopefully, the VSAD will enable researchers to better understand pro-atherogenic chemical responses and identify potential therapeutic solutions to combat the number one killer of Americans.

REFERENCES

[1] S. L. Murphy, J. Xu and K. D. Kochanek, "Deaths: Final Data for 2010," *National Vital Statistics Reports,* vol. 61, no. 4, pp. 1-117, 2013.

[2] U.S. Department of Health and Human Services, "Fact Book Fiscal Year 2012," National Institutes of Health: Heart, Lung, & Blood Institute, 2013.

[3] "Forecasting the Future of Cardiovascular Disease in the United States: A Policy Statement from the American Heart Association," *Circulation,* no. 123, pp. 933-944, 2011.

[4] A. S. Go, D. Mozaffarian and V. L. Roger, "Heart Disease and Stroke Statistics—2013 Update: A Report from the American Heart Association," *Circulation,* vol. 127, pp. 6-245, 2013.

[5] S. Hammer, A. Jeays and P. L. Allan, "Acquisition of 3-D Arterial Geometries and Integration with Computational Fluid Dynamics," *Ultrasound in Med. & Biol.,* vol. 35, no. 12, pp. 2069-2083, 2009.

[6] T. D. Brown, "Techniques for Mechanical Stimulation of Cells In Vitro: A Review," *J. Biomech,* vol. 33, no. 1, pp. 3-14, 2000.

[7] J. E. Moore, E. Burki and A. Suciu, "A Device for Subjecting Vascular Endothelial Cells to Both Fluid Shear Stress and Circumferential Cyclic Stretch," *Annals of Biomedical Engineering,* vol. 22, pp. 416-422, 1994.

[8] C. A. Davis, S. Zambrano, P. Anumolu, A. Allen, L. Sonoqui and M. Moreno, "Device-based In Vitro Techniques for Mechanical Stimulation of Vascular Cells: A Review," *Journal of Biomechanical Engineering,* 2014.

[9] J. H. Haga, Y.-S. J. Li and S. Chien, "Molecular basis of the effects of mechanical stretch on vascular smooth muscle cells," *Journal of Biomechanics,* vol. 40, no. 5, pp. 947-960, 2007.

[10] Y.-S. J. Li, J. H. Haga and S. Chien, "Molecular basis of the effects of shear stress on vascular endothelial cells," *Journal of Biomechanics,* vol. 38, no. 10, pp. 1949-1971, 2005.

[11] D. E. Berardi and J. M. Tarbell, "Stretch and Shear Interactions Affect Intercellular Junction," *Cellular and Molecular Bioengineering,* vol. 2, no. 3, pp. 320-331, 2009.

[12] T. Thacher, R. F. Da Silva and N. Stergiopulos, "Differential Effects of Reduced Cyclic

Stretch and Perturbed Shear Stress Within the Arterial Wall and on Smooth Muscle Function," *American Journal of Hypertension,* vol. 22, no. 12, pp. 1250-1257, 2009.

[13] X. Peng, F. A. Recchia, B. J. Byrne, I. S. Wittstein, R. C. Ziegelstein and D. A. Kass, "In Vitro System to Study Realistic Pulsatile Flow and Stretch Signaling in Cultured Vascular Cells," *American Journal of Physiology,* vol. 279, no. 3, pp. C797-C805, 2000.

[14] Y. Qiu and J. M. Tarbell, "Numerical Simulation of Pulsatile Flow in a Compliant Curved Tube Model of a Coronary Artery," *Journal of Biomechanical Engineering,* vol. 122, no. 1, pp. 77-85, 1999.

[15] J. W. Krueger, D. F. Young and S. C. Cholvin, "An In Vitro Study of Flow Response by Cells," *Journal of Biomechanics,* vol. 4, no. 1, pp. 31-34, 1971.

[16] J. D. Humphrey and S. L. Delange, An Introduction to Biomechanics: Solids and Fluids, Analysis and Design, New York: Springer, 2004.

[17] L. Huang, P. S. Mathieu and B. P. Helmke, "A Stretching Device for High-Resolution Live-Cell Imaging," *Ann. Biomed. Eng.,* vol. 38, no. 5, pp. 1728-1740, 2010.

[18] S. Zhao, A. Suciu, T. Ziegler, J. E. Moore, E. Burki, J. Meister and H. R. Brunner, "Synergistic Effects of Fluid Shear Stress and Cyclic Circumferential Stretch on Vascular Endothelial Cell Morphology and Cytoskeleton," *Arteriosclerosis, Thrombosis, and Vascular Biology,* no. 15, pp. 1781-1786, 1995.

[19] D. N. Ku and D. P. Giddens, "Hemodynamics of the Normal Human Carotid Bifurcation: In Vitro and In Vivo Studies," *Ultrasound in Medicine & Biology,* vol. 11, no. 1, pp. 13-26, 1985.

[20] S. Chien, "Mechanotransduction and endothelial cell homeostasis: the wisdom of the cell," *American Journal of Physiology - Heart and Circulatory Physiology,* vol. 292, no. 3, pp. H1209-H1224, 2007.

[21] W. O. Lane, A. E. Jantzen, T. A. Carlon, R. M. Jamiolkowski, J. E. Grenet and M. M. Ley, "Parallel-plate Flow Chamber and Continuous Flow Circuit to Evaluate Endothelial Progenitor Cells under Laminar Flow Shear Stress," *Journal of Visualized Experiments,* p. 59, 2012.

[22] C. Wang, L. Hao and M. A. Schwartz, "A Novel In Vitro Flow System for Changing Flow Direction on Endothelial Cells," *Journal of Biomechanics,* vol. 45, no. 7, pp. 1212-1218, 2012.